Preparation of prussian blue nanoparticles with single precursor

Zhiqian Jia[*], Genban Sun

College of Chemistry, Beijing Normal University, Beijing 100875, PR China

Abstract

$Fe_4[Fe(CN)_6]_3$ nanoparticles were prepared with potassium ferrocyanide as the single precursor. The effects of precursor concentration and temperature on the particles were investigated. The reaction mechanism was explained. Calculation showed that formation of $Fe_4[Fe(CN)_6]_3$ precipitates and volatile HCN greatly reduce the electron potential of Fe^{3+}/Fe^{2+} and increase the reaction extent of the oxidation of ferrous ions.
© 2007 Elsevier B.V. All rights reserved.

Keywords: Synthesis; $Fe_4[Fe(CN)_6]_3$; Prussian blue; Nanoparticles; Single precursor; Reverse microemulsion

1. Introduction

Prussian Blue (PB) and its analogues form an important class of insoluble, mixed-valence compounds, and have applications in magnetic materials [1,2], molecular sieves [3], catalysis, solid-state batteries, biosensors [4] and molecular magnets [5]. The methods of microemusions [6], poly(vinylpyrrolidone) protection [7], electrodepositing technology [8] and apoferritin cage [9] have been employed to synthesize nanoparticles or nanowire arrays of PB analogues.

In the preparation of nanosized particles with liquid precipitation methods, supersaturation and its distribution play important roles in determining the resultant particle morphology and size distribution. If supersaturation is too high, agglomeration will become an important growth mechanism, leading to irregular agglomerates [10]. Supersaturation distribution in a reaction system mainly affects the particles size distribution. Moderate supersaturation with good distribution can be obtained by generating precipitation ions through chemical reactions [11], e.g., decomposition of compounds, hydrolysis of metal alkoxides, conversion of metal complexes [12].

In this paper, $Fe_4[Fe(CN)_6]_3$ nanoparticles were prepared with potassium ferrocyanide as the single precursor. The slow dissociation of the $[Fe(CN)_6]^{4-}$ complex ensures a limited concentration of free ferrous ions and consequently controlled supersaturation in the formation of PB nanoparticles. The method is simple and convenient. The effects of precursor concentration and reaction temperature on the particles were studied. Calculation of electron potential was given to provide an insight into the reaction mechanism. For comparison, PB nanoparticles were also prepared with the reverse microemulsion method.

2. Experimental

In the syntheses, hydrogen chloride acid solution was added into the $K_4Fe(CN)_6$ solution in the test-tube and mixed. After reaction, the sol was centrifuged and washed with distilled water for three times. The morphology of the as-obtained particles was observed with transmission electron microscopy (TEM, HITACHI H800, Japan). The absorbance was scanned with UV–vis spectrophotometer (Cintra 10e, Australia). XRD pattern was analyzed with monochromatized Cu Kα incident radiation (Shimadzu XRD-6000). All the chemical reagents, including $K_4Fe(CN)_6$, hydrogen chloride acid, cyclohaxane, amyl alcohol and cetyltrimethyl ammonium bromide (CTAB), were analytical grade.

3. Results and discussion

To explore the effects of the precursor concentration, $K_4Fe(CN)_6$ solutions of $0.0025\,mol\,l^{-1}$, $0.0125\,mol\,l^{-1}$ and $0.025\,mol\,l^{-1}$, with same hydrogen chloride acid concentration ($1.6\,mol\,l^{-1}$), were used as precursors, respectively. At $25\,°C$, the solutions appeared light blue after 3 days and became

* Corresponding author. Tel.: +86 10 58210560.
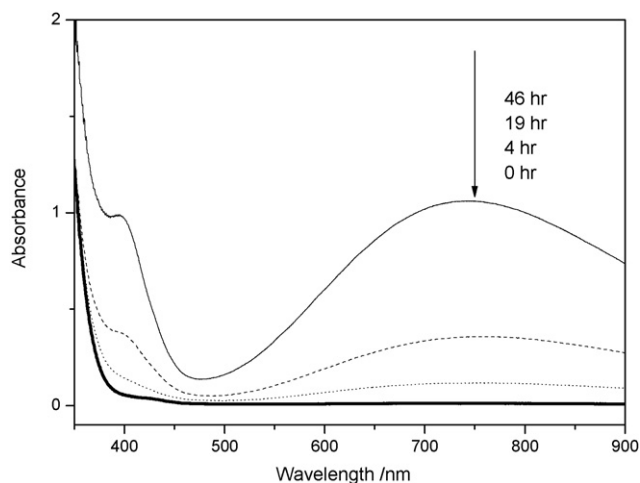 *E-mail address:* zhqjia@bnu.edu.cn (Z. Jia).

Fig. 1. Absorbance of precursor solution (0.0125 mol l^{-1} K$_4$Fe(CN)$_6$ and 1.6 mol l^{-1} hydrogen chloride acid) with time.

Fig. 3. XRD pattern of the particles obtained at 25 °C.

deep blue at the 5th day. From the evolution of the absorbance of the precursor solution (Fig. 1), it could be seen that the broad band centered at 710 nm, which is consistent with an inter-metal charge-transfer band from Fe^{2+} to Fe^{3+} in PB [13], increased with the time. At the 5th day, the sol were centrifuged and analyzed with TEM. The results showed that with the increased K$_4$Fe(CN)$_6$ concentration from 0.0025 mol l^{-1} to 0.025 mol l^{-1}, the particles decreased slightly from 50 nm to 30 nm in size (Fig. 2a–c). The selected area electron diffraction (SAED) showed that all the particles were polycrystalline. X-ray powder diffraction analysis of the as-obtained particles
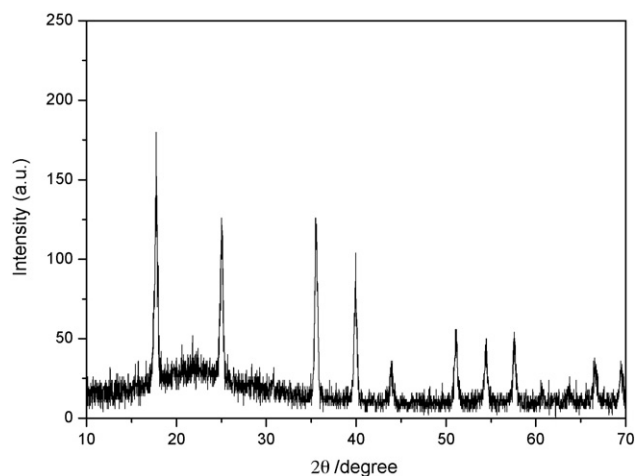
(Fig. 3) showed peaks at 17.5° (2 0 0), 24.8° (2 2 0), 35.4° (4 0 0), 39.8° (4 2 0), 43.7° (4 2 2), 50.96(4 4 0), 54.3(6 0 0), 57.5(6 2 0), 66.5(6 4 0) and 69.4(6 4 2), which can be indexed as the PB cubic space group *Fm3m* [14].

For K$_4$Fe(CN)$_6$ solution of 0.025 mol l^{-1}, when the reaction temperature was increased to 60 °C, the precursor solutions appeared light blue after 1 h and became deep after 3 h. The as-prepared particles were cube-shaped, about 500 nm in size (Fig. 2d). At 90 °C, the particles grew to about 1 μm due to the high growth rate at high temperature. When triton X-100 (2 × 10^{-4} mol l^{-1}) and CTAB (2 × 10^{-4} mol l^{-1}) were used as protectors in the precursor solution (0.025 mol l^{-1} K$_4$Fe(CN)$_6$,
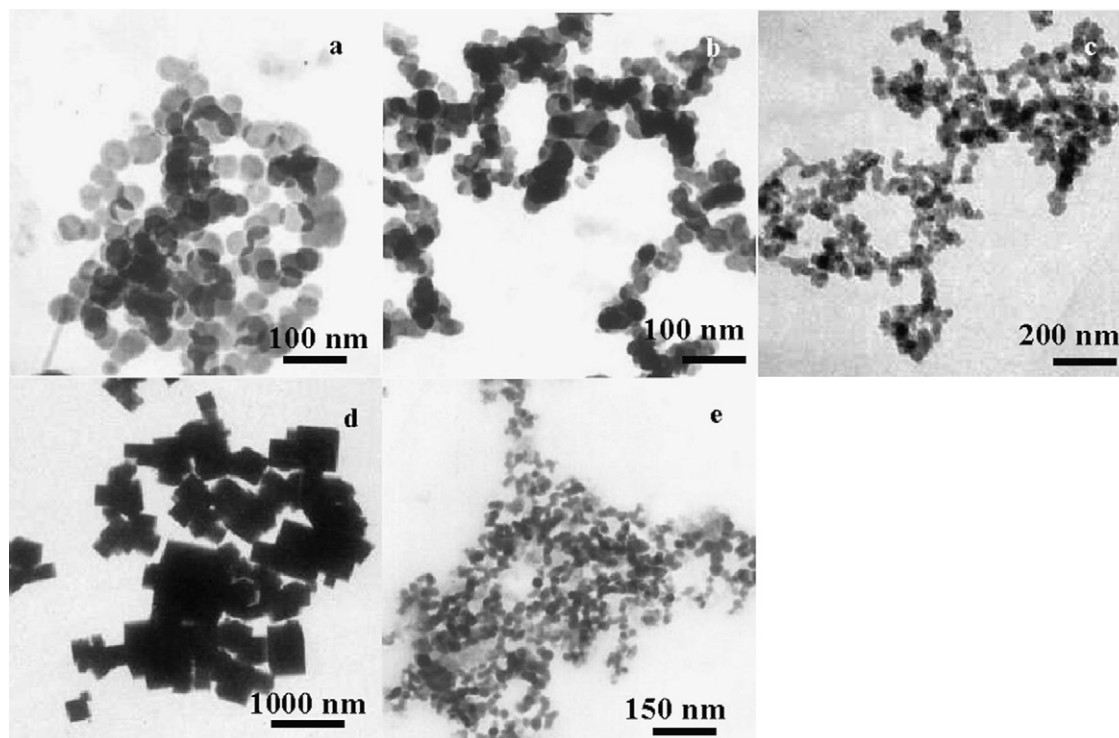
Fig. 2. TEM images of particles. (a) 0.0025 mol l^{-1} K$_4$Fe(CN)$_6$ solution, 25 °C. Inserted is SAED of the particles, (b) 0.0125 mol l^{-1} K$_4$Fe(CN)$_6$ solution, 25 °C, (c) 0.025 mol l^{-1} K$_4$Fe(CN)$_6$ solution, 25 °C, (d) 0.025 mol l^{-1} K$_4$Fe(CN)$_6$ solution, 60 °C, and (e) prepared with reverse emulsion method.

1.6 mol l^{-1} hydrogen chloride acid), white precipitates appeared at once probably due to the electrostatic interaction between protonized triton X or CTAB cations and $[Fe(CN)_6]^{4-}$ anions. Sodium dodecylsulfonate (1.8×10^{-4} mol l^{-1}) was found to have no apparent effects on the growth of particles.

For comparison, $Fe_4[Fe(CN)_6]_3$ particles were also prepared with reverse microemulsion method. The transparent microemulsion of A contained 10 ml cyclohaxane, 0.5 ml amyl alcohol, 6 mmol l^{-1} CTAB and 21.6 µl 0.025 mol l^{-1} FeCl$_3$. The microemulsion of B contained 21.6 µl 0.0188 mol l^{-1} K$_4$Fe(CN)$_6$, and the concentrations of cyclohaxane, amyl alcohol and CTAB were same as that of the microemulsion A. The value of [H$_2$O]/[CTAB] in the two microemulsions equaled 20. Then the two kinds of microemulsion were mixed and stirred for 17 h at 50 °C. The obtained particles were about 35 nm in size (Fig. 2e).

The above results showed that the single precursor method is simple and convenient in operation. As for the reaction mechanism is concerned, in the precursor solutions, K$_4$Fe(CN)$_6$ can dissociate into Fe^{2+} and CN$^-$ ions [15].

$$[Fe(CN)_6]^{4-} \rightleftharpoons 4CN^- + FeCN_2 \tag{1}$$

$$FeCN_2 \rightleftharpoons Fe^{2+} + 2CN^- \tag{2}$$
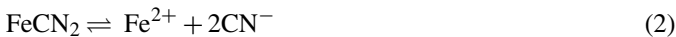
Reactions (1) and (2) can be combined into one equation:

$$[Fe(CN)_6]^{4-} \rightleftharpoons 6CN^- + Fe^{2+} \tag{3}$$
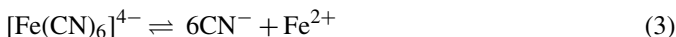
Fe^{2+} may be oxidized into Fe^{3+} by the air.

$$4Fe^{2+} + O_2 + 4H^+ = 4Fe^{3+} + 2H_2O \tag{4}$$
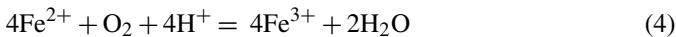
Eq. (4) can be written as two half cell reactions:

$$O_2 + 4H^+ + 4e = 2H_2O \tag{5}$$

$$Fe^{2+} - e = Fe^{3+} \tag{6}$$

Then Fe^{3+} reacts with $[Fe(CN)_6]^{4-}$ and forms Fe$_4$[Fe(CN)$_6$]$_3$ blue precipitates. In acidic solution, CN$^-$ reacts with H$^+$ and generates volatile HCN.

$$4Fe^{3+} + 3[Fe(CN)_6]^{4-} = Fe_4[Fe(CN)_6]_3 \downarrow \tag{7}$$

$$CN^- + H^+ \rightleftharpoons HCN \tag{8}$$

The formation of PB precipitates and HCN move Eq. (3) to the right side, and also reduce the electron potentials of Eqs. (5) and (6) as shown below.

For Eq. (5), at 25 °C,

$$E_1 = E_1^\circ + \left(\frac{0.059}{4}\right) \lg(P_{O_2} \alpha_{H^+}{}^4) \tag{9}$$

where E_1° is the standard potential ($E_1^\circ = 1.229$ v), P_{O_2} the partial pressure of O$_2$ in the air, and α_{H^+} is the activity of H$^+$. When $P_{O_2} = 0.29$ atm and $\alpha_{H^+} = 1$ mol l^{-1}, $E_1 = 1.149$ v.

For Eq. (6), at 25 °C,

$$E_2 = E_2^\circ + 0.059 \lg \left(\frac{\alpha_{Fe^{3+}}}{\alpha_{Fe^{2+}}}\right) \tag{10}$$

Herein $E_2^\circ = 0.771$ v, $\alpha_{Fe^{3+}}$ and $\alpha_{Fe^{2+}}$ are the activities of Fe^{3+} and Fe^{2+}, respectively.

$$\alpha_{Fe^{3+}} = \left(\frac{k_{ap}}{\alpha_{[Fe(CN)_6]}^3}\right)^{1/4} \tag{11}$$

where k_{ap} is the activity product of Fe$_4$[Fe(CN)$_6$]$_3$, $\alpha_{Fe(CN)_6}$ is the activity of $[Fe(CN)_6]^{4-}$. $\alpha_{Fe^{2+}}$ can be obtained from the equilibrium constant, K, of Eq. (3).

$$K = \frac{\alpha_{Fe^{2+}} \alpha_{CN}{}^6}{\alpha_{Fe(CN)_6}} \tag{12}$$

Herein $K = 10^{-35.4}$. [16] Eq. (8) may be regarded as the side reaction of Eq. (3). The side reaction coefficient, $\kappa_{CN(H)}$ is expressed as:

$$\kappa_{CN(H)} = \frac{\alpha_{CN'}}{\alpha_{CN}} = 1 + \alpha_{H^+} \beta \tag{13}$$

where $\alpha_{CN'}$ is the concentration of CN$^-$ anions not coordinated with Fe^{2+}, α_{CN} is that of the free CN$^-$ anions, and β is the formation constant of HCN ($\beta = 10^{9.2}$). Apparently, in acidic and neutral conditions, $\kappa_{CN(H)}$ almost equals $\alpha_{H^+} \beta$. Then,

$$\alpha_{CN} = \frac{\alpha_{CN'}}{\kappa_{CN(H)}} = \frac{6 C_{Fe^{2+}} \gamma_{CN}}{\kappa_{CN(H)}} = \frac{6 C_{Fe^{2+}} \gamma_{CN}}{(\alpha_{H^+} \beta)} \tag{14}$$

From Eqs. (12) and (14),

$$\alpha_{Fe^{2+}} = \frac{4.65 K^{1/7} \alpha_{Fe(CN)_6}^{1/7} \kappa_{CN(H)}^{6/7} \gamma_{Fe^{2+}}^{6/7}}{\gamma_{CN}^{6/7}}$$
$$= \frac{4.65 K^{1/7} \alpha_{Fe(CN)_6}^{1/7} \beta^{6/7} \alpha_{H^+}^{6/7} \gamma_{Fe^{2+}}^{6/7}}{\gamma_{CN}^{6/7}} \tag{15}$$

According to Eqs. (11) and (15), Eq. (10) can be rewritten as:

$$E_2 = E_2^\circ + 0.059 \lg(4.65 k_{ap}^{1/4} K^{-1/7} \beta^{-6/7})$$
$$+ 0.059 \lg(\gamma_{CN}^{6/7} \gamma_{Fe^{2+}}^{6/7} \alpha_{Fe(CN)6}^{-25/28} \alpha_{H^+}^{-6/7}) \tag{16}$$

The effects of side reactions on the electrode potential are usually far larger than that of the ionic strength and activity coefficients. [17] When the effects of ionic strength are neglected, Eq. (16) can be simplified as:

$$E_2 = E_2^\circ + 0.059 \lg(4.65 k_{sp}^{1/4} K^{-1/7} \beta^{-6/7})$$
$$+ 0.59 \lg C_{Fe(CN)_6}^{-25/28} C_{H^+}^{-6/7} \tag{17}$$

Herein, k_{sp} is the solubility product of PB ($k_{sp} = 10^{-40.5}$) [16]. Then,

$$E_2 = 0.045 - 0.053 \lg C_{Fe(CN)_6} - 0.051 \lg C_{H^+} \tag{18}$$

Then the formal potential of Fe^{3+}/Fe^{2+} is 0.045 V. The equilibrium constant, K', of Eq. (4) is expressed as:

$$\lg K' = \frac{4(E_1 - E_2)}{0.059} \tag{19}$$

When $E_1 = 1.222$ V and $E_2 = 0.045$ V, lg K' is 79.5. With the increased $K_4Fe(CN)_6$ concentration from 0.0025 mol l^{-1} to 0.0125 mol l^{-1} and 0.025 mol l^{-1}, E_2 increases slightly from -1.03 V to -0.066 V and -0.050 V, and lg K' decreases from 89.8 to 87.3 and 86.2. It seemed that the smaller particles obtained at higher $K_4Fe(CN)_6$ concentration (Fig. 2a–c) should mainly resulted from the higher supersaturation.

Notifying that E_2° is 0.771 V and the corresponding equilibrium constant lg K' is 30.6, the precipitation reaction (7) and side reaction (8) greatly decrease the potential of Eq. (6) and increase the reaction extent of Eq. (4).

4. Conclusions

This paper reported the preparation of $Fe_4[Fe(CN)_6]_3$ nanoparticles with potassium ferrocyanide as the single precursor. Calculation of electron potential was also given to provide an insight into the reaction mechanism. The formation of PB precipitates and HCN move the dissociation of ferrocyanide to the right side, and also apparently reduce the potential of Fe^{3+}/Fe^{2+}. With the increased $K_4Fe(CN)_6$ concentration, the particles size decreased. Compared with the reverse microemulsion method, the single precursor method is simple and convenient.

Acknowledgements

References

[1] P.H. Zhou, D.S. Xue, H.Q. Luo, X.G. Chen, Nano Lett. 2 (2002) 845.
[2] P.A. Berseth, J.J. Sokol, M.P. Shores, J.L. Heinrich, J.R. Long, J. Am. Chem. Soc. 122 (2000) 9655.
[3] M. Pyrasch, A. Toutianoush, W.Q. Jin, J. Schnepf, B. Tieke, Chem. Mater. 15 (2003) 245.
[4] D. Moscone, D. D'Ottavi, D. Compagnone, G. Palleschi, A. Amine, Anal. Chem. 73 (2001) 2529.
[5] J.T. Culp, J.H. Park, D. Stratakis, M.W. Meisel, D.R. Talham, J. Am. Chem. Soc. 124 (2002) 10083.
[6] V. Sebastien, M. Li, M. Stephen, Synthesis of Prussian Blue nanoparticles and nanocrystal superlattices in reverse microemulsions, Angrew. Chem. Int. Ed. 39 (2000) 1793–1796.
[7] U. Takashi, K. Susumu, Prussian Blue nanoparticles protected by poly(vinylpyrrolidone), J. Am. Chem. Soc. 125 (2003) 7814–7815.
[8] P.H. Zhou, D.S. Xue, H.Q. Luo, X.G. Chen, Fabrication, structure and magnetic properties of highly ordered Prussian Blue nanowire arrays, Nano. Lett. 2 (8) (2002) 845–849.
[9] M. D.-V. Jose, C. Enrique, Nanoparticles of Prussian Blue ferritin: a new riute for obtaining nanoparticles, Inorgan. Chem. 42 (2003) 6983–6985.
[10] J.A. Dirksen, T.A. Ring, Fundamentals of crystallization: kinetic effects on particle size distributions and morphology, Chem. Eng. Sci. 46 (1991) 2389.
[11] Tadao Sugimoto, Preparation of monodispersed colloidal particles, Adv. Colloid Interf. Sci. 28 (1987) 65.
[12] T. Sugimoto, S. Chen, A. Muramatsu, Colloid. Surf. A: Physicochem. Eng. Aspects 135 (1998) 207.
[13] M.B. Robin, Inorg. Chem. 1 (1962) 337.
[14] H.J. Buser, D. Schwarzenbach, W.L. Petter, Inorg. Chem. 16 (1977) 2704.
[15] S.C. Chen, Important Inorganic Reactions, Shanghai Science and Technology Press, 1982.
[16] John A.D., Lange's Handbook of Chemistry, 14th ed., McGraw-Hill, Inc., 1992.
[17] J.S. Fritz, Quantitative Analytical Chemistry, 4th ed., Allyn and Bacon, 1979.